

CONSTRUCTION AND FUNCTIONING OF AN EFFICIENT ULTRASONIC ATOMIZER

Dragan Šarković and Vukota Babović

Faculty of Science, P. O. Box 60, 34000 Kragujevac, Yugoslavia

(Received December 5, 2001)

ABSTRACT - We report on the construction of an efficient ultrasonic atomizer. The main piece of the apparatus is the ceramic transducer working at frequency of 1.7 MHz, with power of nearly 12W supplied by a standard oscillating circuit of the Misner type. Atomizer impedance vs. frequency figures are examined in details. In a number of experiments we have tested the atomizer producing water aerosols. The efficiency of our liquid dropper could be as high as 30 milliliters pro minute. Preliminary results show aerosols are of fine quality. The mean droplet diameter is estimated of the order of several microns. Searching for an auxiliary tool potentially suitable in statistical analyzes of produced clouds, we propose a peculiar density function of diameters distribution. This analytical expression seems to be widely applicable and beside could be generalized for a class of low-viscous liquids. We believe the atomizer is the successful pace toward the realization of an idea concerning applications of aerosols in tobacco industry; details of that project could in future be the subject of a patent and so must be omitted here.

1. INTRODUCTION

The method of ultrasonic spraying of liquids was invented by Wood and Loomis in the third decade of the last century [16]. This controllable process of tiny droplets production by means of strong high frequency sound fields could be understood, as shown by Eisenmenger [6], on the base of the well known capillary wave theory. Generally, droplets ejected on a free surface of a liquid stem from vertical oscillations of liquid particles (Faraday excitation, a 'robust phenomenon' [10] observed in liquids with over a two decade range in frequency). Capillary surface waves suffer the transition to droplet-ejecting states after the increasing the applied forcing; the Rayleigh instability [3b] causes wave peaks to break up into droplets. In fact, as subsequent investigations confirm, two notable physical effects are to be mention, at least in high frequency experiments, as causes of the effect: surface waves and cavitation [5].

After the pioneering discovery, a number of authors (e.g. [1], [12], [15]) developed various ultrasonic sprayers, indicating in theirs experiments some of its potentially interesting scientific, medical and engineering applications. The including of various piezoceramic materials famous for excellent combination of relevant electrical, mechanical and thermodynamical features made it possible for scientists to increase main atomizer performances, first of all the efficiency of droplets production. In this field, further progress was notice-able in late sixtieth ([4], and references cited therein). In subsequent years and decades, up to ours days, one can follow the steady interest in scientific literature for developments and applications of droplet-ejection projects.

In this paper we describe the construction and operation of an ultrasonic atomizer, which proved to be very efficient in scattering water and other liquids. Section 2 gives details of construction and also deals with the electrical scheme applied in our high frequency oscillator. In Section 3 we present experimental results of HF sprayer operation. After reviewing in short the physical mechanisms of controllable drops production process, we concern in Section 4 some features of the

given artificial mist and the reader could find the preliminary data on physical characteristics such as mean diameter of droplets, as well as some useful formulae of general importance in proceedings the basic performance of the apparatus. Finally, there are concluding comments in Section 5 on overall set-up performances and expected perspectives in further development of our ultrasonic system. The main text is accompanied by an Appendix, thought-out to make the reader's job in hydrodynamic wave equations easier.

2. CONSTRUCTION AND ELECTRICAL SCHEME

a) Construction

Our atomizer uses a piezoceramic transducer having the form of a thin circular plate. Dimensions of this disc are 20 mm (diameter) and 1.2 mm (depth). Each circular surface of the transducer is metallized. The material used is known under the secret code "SP 8" and has been made by German firm "Ceramtec".

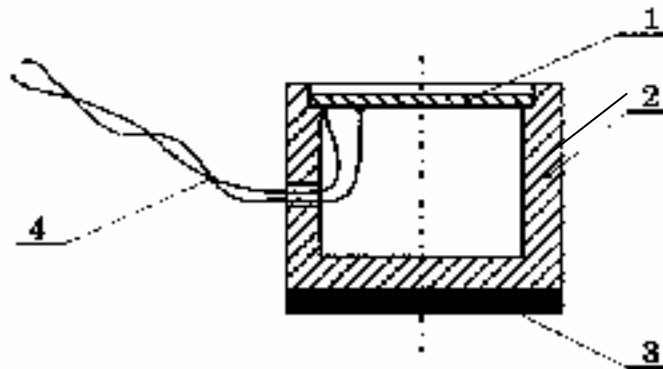


Fig. 1 Ultrasonic transducer 1.7 MHz (vertical section); 1 – piezoceramic plate; 2 – chamber (hollow Teflon cylinder; 3 – weight (stabilizing disc); 4 – current lead-ins

The piezoceramic plate is situated on the upper base of a hollow cylinder made of Teflon; the lower base of the cylinder is accompanied by a weight (procron disc) which enables a stable position of the whole element meant to operate at the bottom of a container.

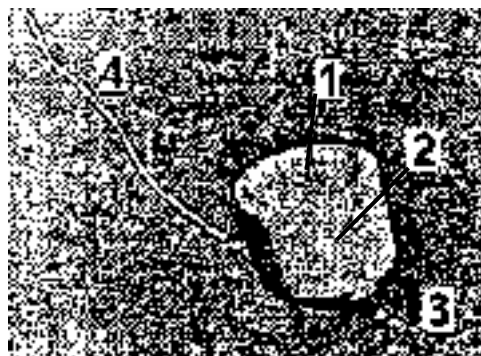


Fig. 2 Ultrasonic transducer 1.7 MHz (photograph); 1 – piezoceramic plate; 2 – chamber (hollow Teflon cylinder; 3 – weight (stabilizing disc); 4 – current lead-ins

Two electrical lead-ins of the transducer are wires assembled of many thin isolated copper fibers; conductors are soldered to metallized surface of the piezoceramic plate.

The vertical section of the transducer is shown on Fig. 1, whereas the photography of the complete piece we see on Fig 2.

b) *Electrical scheme*

We present the scheme (Fig. 3) of an electrical generator, which feeds our electromechanical piezoceramic transducer. The generator can exhibit high frequency electrical oscillations of the order of several megahertz.

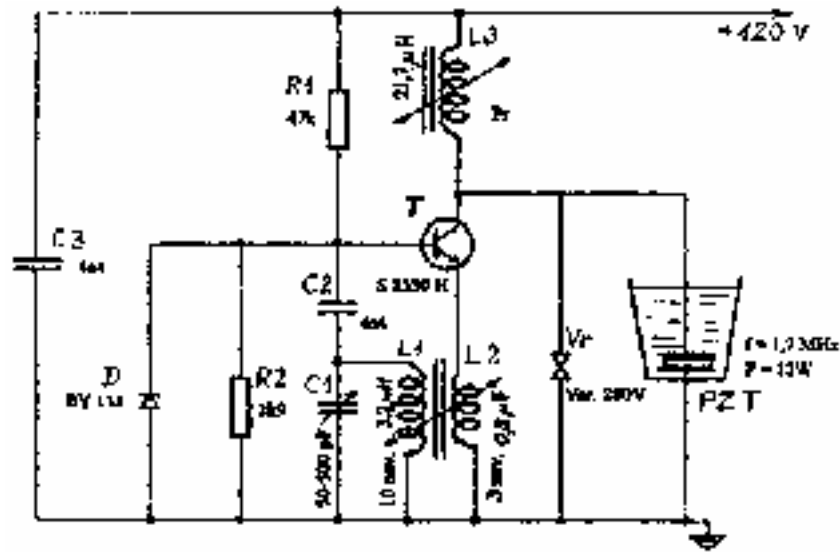


Fig. 3 Electrical circuit of oscillator $F \approx 1.7$ MHz, $P \approx 12$ W

The main electronic component is the transistor S 2530 H, which enables the realization of the oscillating circuit according to one of the standard schemes. As known, S 2530 H is the epitaxial silicon planar power transistor, having the cutoff at $f_t=6$ MHz; with a maximal dissipation of $P_D=90$ W and the electrode voltage of $U_{CE}=400$ V, the transistor in surplus matches the requirements of the used piezoceramic transducer.

As can be easily understood, the oscillator is a self-excited one, of the Misner type; it gains the positive feedback voltage from the own emitter circuit, by means of a pair of mutually coupled inductances and . The theory of the circuit operation is out of the scope of this article; we shall note here only the roles of electronic components constituting the oscillator.

The frequency of the oscillator is determined by the circuit consisted of the variable capacitor C_1 and inductance L_1 modified by a part of the emitter impedance (via the coefficient of the mutual inductance acting between coils L_1 and L_2).

The capacitor C_2 separates the direct base voltage component, which is essential for adjusting of the transistor working point. We remark that this working point is defined by the voltage divider consisting of the resistor R_1 and the combination of the resistor R_2 with the input resistance of the r_b transistor.

The diode D is a limiter of negative half-periods; the base circuit is protected by this diode in cases of too high inverse voltages and currents.

The capacitor C_3 short circuits VF oscillations and in that way eliminates it from the voltage source. In addition, the capacitor reduces eventual environmental radiations.

The varistor V_V protects the transistor in case of uncontrollable voltage jumps.

The coil choke P_r accompanied by the piezoceramic transducer PZT constitutes the impedance which is in fact the output load of the transistor T. Of course, this choke doesn't affect the D.C. operation of the voltage source, but supplies a high VF voltage component needed for transducer feeding. The transistor S 2530 H output provides the input power of the piezoceramic transducer.

The oscillator uses a stabilized voltage $U=120$ V. (Our kit includes the rectifier 6443 B dc power Hewlett-Packard supply.)

In many tests, we have convinced ourselves of the reliable, stable and reproducible operation of the apparatus.

c) Impedance characteristic

A piezoelectric transducer working on (nearly) mechanical resonant frequency could be thought as having an equivalent circuit scheme consisting of a capacitance C_p in parallel with a serial connection of a capacitance C_r , inductance L and resistance R . The electrical impedance characteristic of a piezoelectric transducer is well known resonant curve shown as an insert on Fig. 5. As a matter of fact we stress that this curve follows from a rather idealized physical model; in praxis, the characteristic is much more complex. In each particular case one has to determine the transducer performances precisely. We have tested our transducer according to a laboratory block-scheme shown on Fig. 4. The measured specimen was fed with current from a function generator (Philips model PM 5133). The response was monitored by means of a X-Y recorder (Packard model 7035 B). We have first recorded a set of $Z=\varphi(F)$ characteristics for an air operation of our transducer. A typical result is presented on Fig. 5.

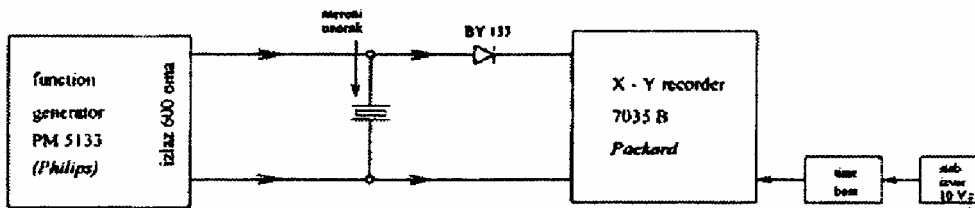


Fig. 4 Block-scheme used for measuring of impedance-frequency characteristics of piezoceramic vibrators

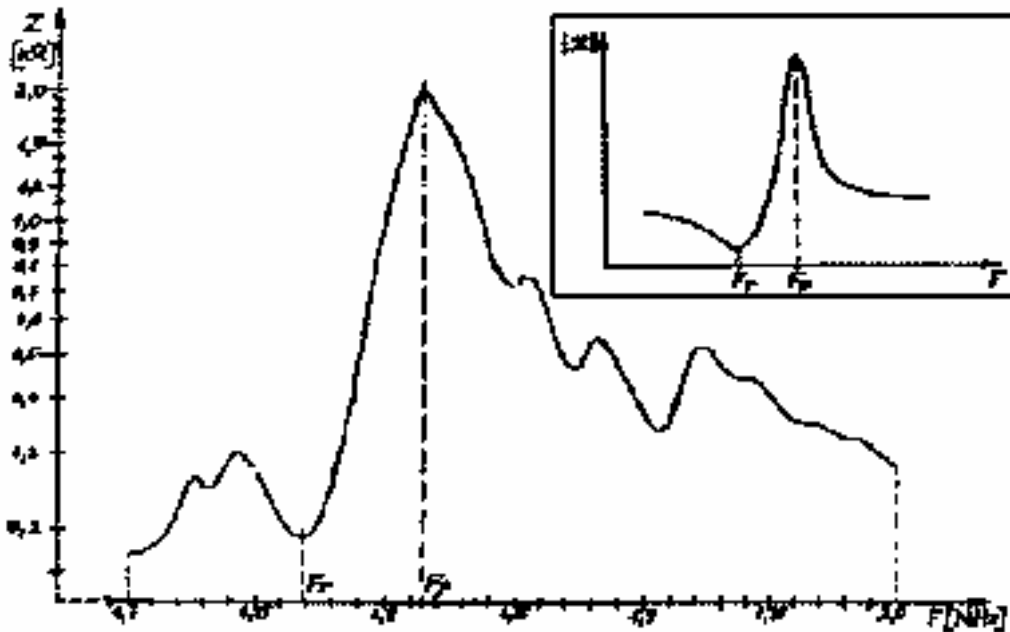


Fig. 5 Impedance-frequency response of the piezoelectric transducer working in air; in insert: idealized characteristic

Besides the minimum (serial resonance) and the maximum (parallel resonance), which are two most pronounce details, the reader can also notice several additional extremes stemming of parasite resonant frequencies. We have concluded that these new appeared peaks have several causes as follows: a) Interferences between direct waves and waves reflected from walls and bottom of the liquid container; b) Deformations of PZT in Teflon cylinder and influences of wire contacts on the metallized surface of PZT; c) Possible imperfections in piezoceramic material.

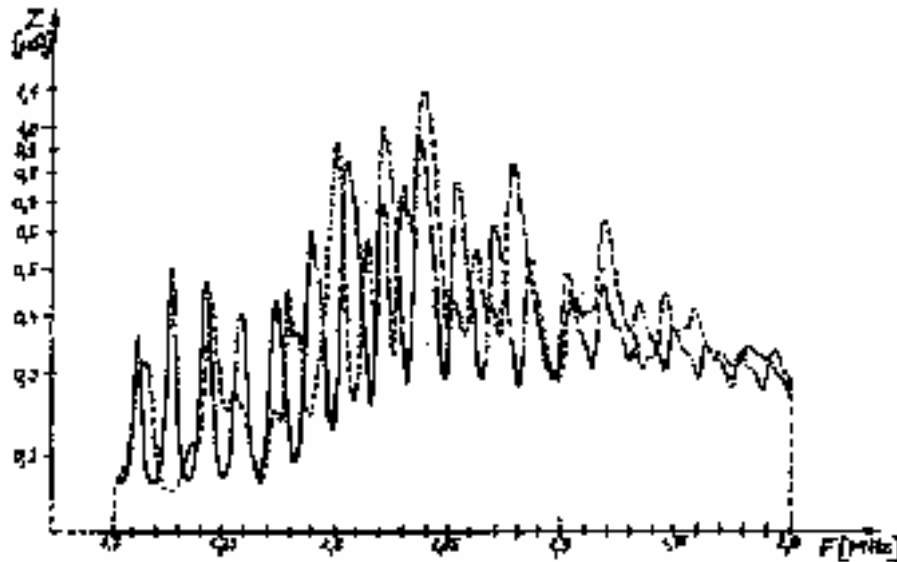


Fig. 6 Impedance-frequency response of the piezoelectric transducer working in water; continuous line for 0.2 l glass tank full of water; dashed line for half-full glass tank

Further, we have put our PZT on the bottom of a glass tank (having the volume $V=0.2$ liters) filled with water first a) not more than half, and then b) till to upper rand. Resulting curves are shown on Fig. 6. The full-line curve (the case a)) is substantially different from the dashed-line curve (the case b)) and both are very dissimilar to the air characteristic given on the previous figure. Numerous parasite frequencies have its causes in already quoted effects as well as in several additional sources: d) Interferences between waves reflected from the free liquid surface and all remained waves in the dynamical regime of apparatus working; e) Formation of waves above the PZT; these change the effective mass of liquid practically being a load of transducer in given moment – transducer vital parameters undergo dynamical modifications.

The impedance characteristics, as we have demonstrated, depend very strongly on the amount of a medium inside which a given ultrasonic atomizer acts. First, we see many resonant peaks not existing in air, and second, we can observe this peaks are very sensitive (changing height and position) on the liquid contents in glass. These characteristics must be carefully considered on the occasion of choosing a working point. During the operation of the atomizer the amount of water (or any other liquid) permanently diminishes, so the characteristic $Z=\varphi(F)$ continuously changes its shape. It means that we could conceive the concept of a working point only as a relative one: evidently, a rapid dynamical process is in question.

3. PRODUCTION OF AEROSOL

The tested ultrasonic atomizer working at $F\approx 1.7$ MHz was positioned at the bottom of the glass container filled with water. The volume of used water was 200 milliliters. The experiment is performed at ambient temperature (18°C). We have activated the generator (Fig. 3) and in a series of tries obtained clouds of droplets, a dense mist, or aerosol (the usual term for a suspension of fine particles in air or gas). The global effect of ultrasonic atomizer is sketched on Fig. 7. The corresponding photographs are shown on Fig. 8.

The overall picture of the process is as follows. According to [10], vertically oscillating ultrasonic driven waves experience a number of bifurcations before the transitions to a droplet-ejecting state (see also [11], and references cited therein.) With increasing forcing, a starting uniform and almost calm surface wave state will evolve into a pronounced standing state. Soon will this go through an aperiodic state often giving large-amplitude waves. The corresponding upward jets tend to break into droplets. In our experiments, which seem to conform this proposed picture, some droplets evidently can be jerk as high as 10 cm above the water surface; in this group one could often detect

sporadic extreme big drops, with diameter up to ~1 mm. Dominant cloud of finest droplets exists near the opening of the container and in close neighborhood aside.

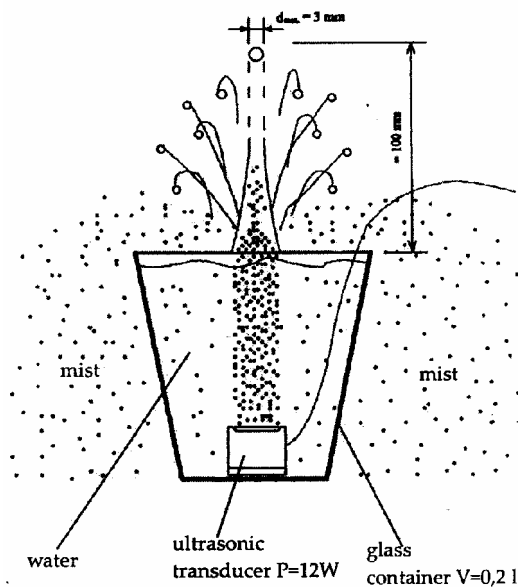


Fig. 7 Schematic view of set-up in a working phase

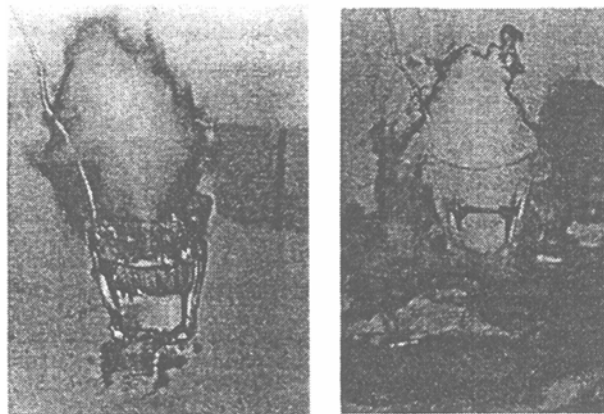


Fig. 8 Photographs of typical atomizer outputs.9

Our atomizer has appeared as an extremely efficient apparatus. It can transform entire volume of water into tiny mist in air for only 5 minutes. Consequently, the efficiency of atomization is

$$A = \frac{0.2 \ell}{5 \text{ min}} = 6.6 \cdot 10^{-7} \text{ m}^3 / \text{s}. \quad (1)$$

This production power is several times greater than powers indicated in earlier literature [4], and comparable with outputs of modern atomizers as presented on Internet by various manufacturers. It is the very point that encourages our efforts just in those ideas we had in the beginning of the job. Namely, the starting impulse for a suitable atomizer realization was the idea of having a powerful ultrasonic source with a perspective to be appropriate for applications in tobacco industries. (We hope, critical details of the planned treatment should be in a near future the subject of a patent and therefore here will be omitted further facts connected with this area of problem.)

4. STATISTICS OF DROPLETS

A) *Water aerosol*

Aerosols, colloidal solutions in gaseous medium (as are water droplets in air), appear in an ultrasonic wave field under the action of two notable physical mechanisms, the sonically induced cavitation and the capillary surface waves. The cavitation theory of ultrasonic aerosol production states that liquid particles scatter and spread around as a result of implosions of cavitation bubbles near the free surface. Although this way of reasoning is surely a regular one, we believe the main direction of the process is connected with standing capillary surface waves. So we will concentrate now ourselves to this topic.

The surface wave theory starts from assumption that the piezoelectric resonator parametrically launches capillary waves on the liquid/air interface. The amplitudes of these waves exponentially grow with the increase of input power and finally droplets broke off from crests of standing waves. The wavelength λ of capillary waves depends (in low-viscous liquids and solutions) on the coefficient of surface tension γ and the mass density ρ according to the known expression

$$\lambda = 2 \sqrt[3]{\frac{\gamma \pi}{\rho F^2}}. \quad (2)$$

Here F stands for the driving frequency of the ultrasonic transducer. For the sake of enhanced understanding of formula, we add an Appendix at the end of this paper in which the reader may find the derivation of the result (2).

The suggested mechanism of droplets generation is stochastic in character. Investigations have shown [14] that the mean diameter of droplets is well correlated with the capillary wavelength if we put $D = \lambda/3$. Using our equation (2) we then obtain

$$D = \frac{2\pi^{\frac{1}{3}}}{3} \left(\frac{\gamma}{\rho F^2} \right)^{\frac{1}{3}}. \quad (3)$$

For water aerosols, one should insert in this expression $\gamma = 0.073$ N/m and $\rho = 1000$ Kg/m³. It gives the following approximate, useful and very simple result:

$$D \approx 4 F^{-\frac{2}{3}}. \quad (4)$$

Starting from this expression one can get a graph shown on Fig. 9. Droplets of several micrometers are likely to be found in water aerosols produced by frequencies of one megahertz.

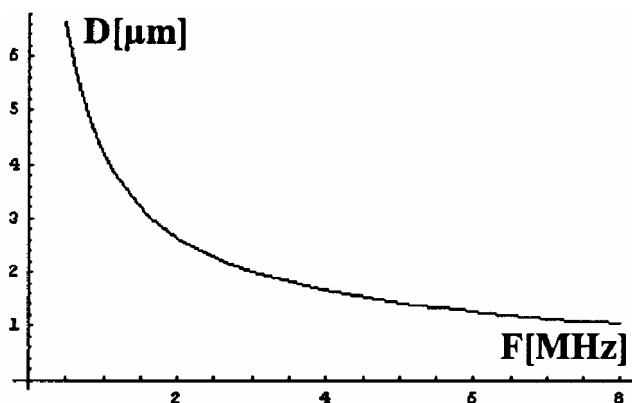


Fig. 9 Mean droplet diameter vs. forcing frequency

Our experimental investigations which are not in conflict with existing literature (cf. with histograms in [4]) show that the density function for the distribution of droplets diameters follows the dependence

$$P(d) = ad^3 e^{-bd}. \quad (5)$$

Parameters of this distribution can be determined in a standard way, first by putting on the condition

$$\int_0^{\infty} P(d) dd = 1. \quad (6)$$

The integral can be evaluated without difficulties and we prove the simple connection

$$a = \frac{b^4}{6}. \quad (7)$$

The mean diameter D is defined in the usual way via the probability function

$$D = \int_0^{\infty} d P(d) dd. \quad (8)$$

Once more the integral can be evaluate in a closed form and we get an another condition of the type

$$D = \frac{24a}{b^5}. \quad (9)$$

Now we readily find how the parameters of distribution can be related to experimental data represented in the measurable quantity D :

$$b = \frac{4}{D}; \quad a = \frac{128}{3} \frac{1}{D^4}. \quad (10)$$

Having in mind (4) we obtain for water the approximate expressions

$$a = \frac{F^{\frac{8}{3}}}{6}; \quad b = F^{\frac{2}{3}}. \quad (11)$$

Finally, the water density function takes the form

$$P(d) = \frac{1}{6} F^{\frac{8}{3}} d^3 e^{-F^{\frac{2}{3}} d}. \quad (12)$$

We stress the significant feature: the probability function only depends on the driving frequency of transducer. Of course, this aspect deserves a short comment. The physical process leading to generation of each drop is rather a complicated event. At least, we must state precisely one important point. The amplitude of oscillatory process should be near the threshold of drops launching. Therefore, we limit the consideration to amplitudes of the order of wavelengths or most frequent diameters of drops. For a driving frequency of one or two megahertz amplitudes should lay below several microns. It also means that the efficiency of aerosol production should not be near its maximal value.

An alternative form of the above expression can be achieved applying the replacement $x=d/D$, i.e. introducing the notion of the reduced diameter. In that case, our equation (12) goes over to the form [take care of the physical condition $P(d)dd=P(x)dx$]

$$P(x) = \frac{128}{3} x^3 e^{-4x}. \quad (13)$$

A three-dimensional plot processed by *Math 4.0* software package, according to above formula, is shown on Fig. 10. The reader can catch sight of some characteristic features of this complex distribution field, including a pronounced maximum.

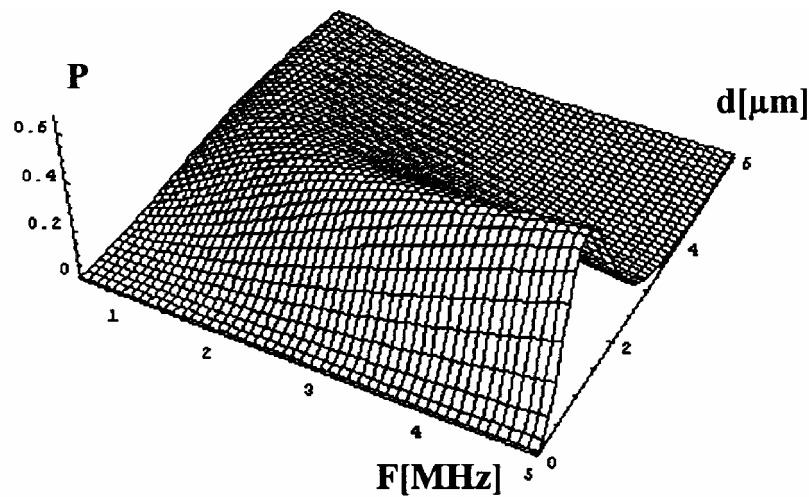


Fig.10 Three-dimensional plot of density function of probability

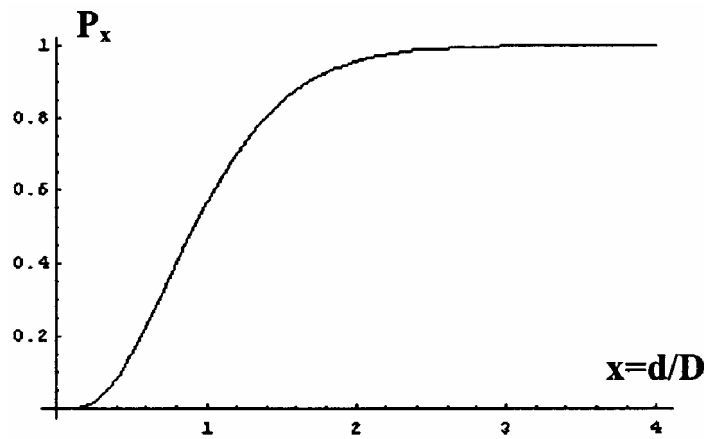


Fig. 11 Integral probability curve

Once knowing the distribution density, we can gain various useful informations. There is a plot on Fig. 11 which gives an integral probability, the percentage of all droplets having the relative diameter less than some fixed number. For example, one could read that nearly % of all droplets is with diameters below 1 50 μm . Negligible number of droplets exceeds in diameter 5 μm . We are aware of fact that this statistics is not very accurate and refers only to a bulk of tiny mist. Nevertheless, we believe the assumed law (5) can reflect main features of our aerosol; it provides a rough estimate very useful in this phase of investigations. The formula (13) really offers a flexible analysis and shall be under our further improvements.

B) Generalization

Now, we shall try to generalize the above results treating any other liquid of a density ρ and surface tension γ . Exceptionally here we use designations ρ_0 and γ_0 for analogous water quantities. Let us introduce a new parameter representing the ratio of density to surface tension (which is the inverse of so-called kinematic surface tension)

$$p = \frac{\rho_r}{\gamma_r}, \quad (14)$$

where $\rho_r = \rho/\rho_0$ and $\gamma_r = \gamma/\gamma_0$. In case of water the corresponding ratio gives $\rho_0/\gamma_0 = 13698.6$, i.e. $p_{\text{water}} = 1$. In other words, the parameter measures the ratio of density to surface tension relative to water. The mean diameter formula takes now the form

$$D = \left(\frac{\gamma_0}{\rho_0 F_r^2} \right)^{\frac{1}{3}}. \quad (15)$$

We conclude that our former equations retain existing form, but we must replace the true frequency with the reduced one defined by $F_r = F\sqrt{p}$. In that way we have for the generalized density function

$$P_r(d) = \frac{1}{6} F_r^{\frac{2}{3}} d^3 e^{-f}, \quad (16)$$

where $f = F_r^{\frac{2}{3}} d$. Let us construct a ratio of two density functions (12) and (16). The result is

$$K \equiv \frac{P(d)}{P_r(d)} = p^{\frac{2}{3}} e^t. \quad (17)$$

The used abbreviation k is defined as

$$k = F^{\frac{2}{3}} d \left(1 - p^{\frac{1}{3}} \right). \quad (18)$$

Table 1 gives relevant data and a comparative survey for several well known liquids. All units are in SI.

Table 1

liquid	density	surface tension	p
Water	1000	0.073	1.00
Glycerine	1200	0.064	1.37
Ethanol	790	0.020	2.88
Castor oil	900	0.035	1.88

We see that the parameter is in all cases greater than unity. The noticeable high ratio is for ethil alcohol 2.88. A plentiful experimental possibility to simulate cases of growing viscosity is in making controllable glycerine-water solutions. Instructive graphs are presented on Fig. 12.

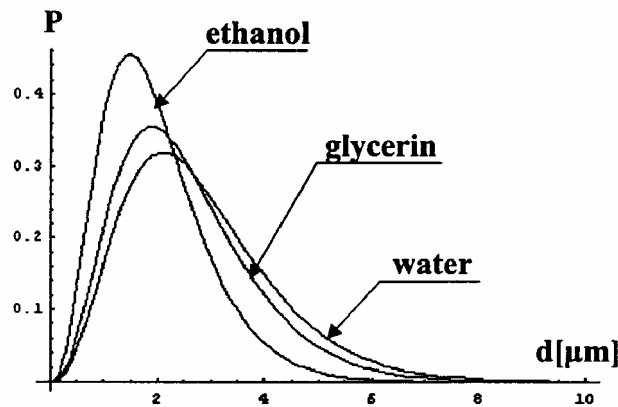


Fig. 12 Comparative review of various density function curves; a) ethanol, b) water, c) glycerin.

We see that an increase of p causes corresponding reductions in number of larger drops. For the same frequency, and equal other common conditions, ethanol mist would be maid of smaller droplets than a water mist. However, we are aware of the fact that this prediction is based on an approximation neglecting viscous effects in liquids. High viscous liquids have droplet formation thresholds which depend on only viscosity, as evidenced in [10]. Nevertheless, we believe that low-viscous fluids mostly demonstrate features sketched on Fig 12.

5. CONCLUSION

In this paper we have reported on the construction of an efficient ultrasonic piezoceramic transducer. The apparatus appears as a robust producer of ample homogeneous clouds of micron droplets. Our experiments are supplementary evidences that the phenomenon of droplet-ejecting capillary waves works well in megahertz regions.

We have proposed an auxiliary function representing the density distribution of droplet size probability. This function which works in agreement with main from experiments emerging facts, could be a significant tool in various physical characterizations of aerosols. We have tried to apply the density function for rough predictions of results in cases when a liquid under consideration has the density-to-tension ratio which exceeds the corresponded value of water. The preliminary data seem to be correct for low-viscous media.

Finally, we believe that the entire project of our ultrasonic atomizer construction gives initial encouraging results which could lead in future toward a desired application of the apparatus in tobacco industry.

6. APPENDIX: DISPERSION RELATION

Let us consider an amount of water (or any other liquid) in a container of rectangular shape. (The shape, as we shall see, plays no role at all: waves have so small wavelengths that any effects due to boundary conditions or meniscus interactions are negligible.) The initial height of water layer is h , see Fig A1.

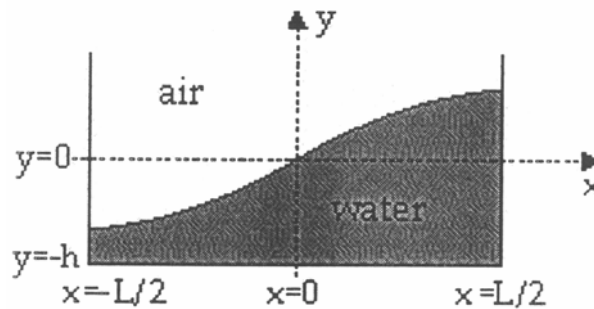


Fig. A1 Considering liquid oscillations in a rectangular container

Let us imagine the surface of fluid supports a harmonic standing wave. We will analyze this oscillating system. The following initial assumptions are considered as true: a) amplitudes of waves are small and b) the viscosity of fluid is negligible.

An oscillating particle at a given position $M(x, y)$ has a displacement \vec{s} in a moment t and holds the relation

$$\vec{s}(x, z, t) = \vec{i}s_x(x, z, t) + \vec{j}s_y(x, z, t). \quad (\text{A1})$$

The vertical displacement having a knot in the co-ordinate origin can be written as follows

$$s_y(x, z, t) = f(y) \cos \omega t \sin kx. \quad (\text{A2})$$

Here the function $f(y)$ is temporary unknown and shall be later determined. Now we take into consideration the boundary condition on the container wall. For $x=\pm L/2$ the oscillation of fluid particle can have only a vertical component. It means that the horizontal displacement must be of the form

$$s_x(x, z, t) = g(y) \cos \omega t \cos kx. \quad (\text{A3})$$

Here we have another transversal component designated as $g(y)$. The further analysis goes hypothesizing no divergence in the system.

$$\nabla \cdot \vec{s} = 0. \quad (\text{A4})$$

as well as annulling all whirl components

$$\nabla \times \vec{s} = 0. \quad (\text{A5})$$

Now, from (A4) we easily get

$$-k g(y) + \frac{df(y)}{dy} = 0, \quad (\text{A6})$$

whereas the equation (A5) yields

$$k f(y) - \frac{dg(y)}{dy} = 0. \quad (\text{A7})$$

The combination of (A6) and (A7) gives the differential equation

$$\frac{d^2 f(y)}{dy^2} - k^2 f(y) = 0. \quad (\text{A8})$$

In addition, we see that holds as well the differential equation for the function g :

$$-\frac{d^2 g(y)}{dy^2} + k^2 g(y) = 0. \quad (\text{A9})$$

From (A8) immediately follows $f(y) = Ae^{ky} + Be^{-ky}$. In a similar way, from (A9) we find $g(y) = Ae^{ky} - Be^{-ky}$. Integration constants A and B are mutually related because of boundary conditions acting at the container bottom; there cannot be any kind of vertical movements. This requirement, i.e. the condition $s(-h) = 0$, evidently is identical with $f(y) = 0$ when $y = -h$. So we get $2kh$

$$B = -Ae^{-2kh}. \quad (\text{A10})$$

Equations (A2) and (A3) can now be rewritten as

$$s_x = A(e^{ky} + e^{-2kh}e^{-ky}) \cos \omega t \cos kx, \quad (\text{A11})$$

$$s_y = A(e^{ky} - e^{-2kh}e^{-ky}) \cos \omega t \sin kx. \quad (\text{A12})$$

These equations give a detailed description of particle movements. Trajectories are straight lines in x-y plane. The above formulae are simpler for a thick liquid layer because the factor $\text{Exp}(-2kh)$ could be omitted; waves appear as a purely surface phenomenon, with harmonic variations in horizontal direction and exponential decay in vertical direction. One could estimate the depth δ of sound field in accordance with the condition $k\delta \approx 1$, i.e. $\delta = \lambda/2$; so the deep water criterion could be adopted to read $h > \delta$.

The gravitational as well as surface tensions effects are in treated oscillating processes the primary restoring forces. As far as the surface tension is concerned we should elaborate main ideas looking a sketch on Fig A2.

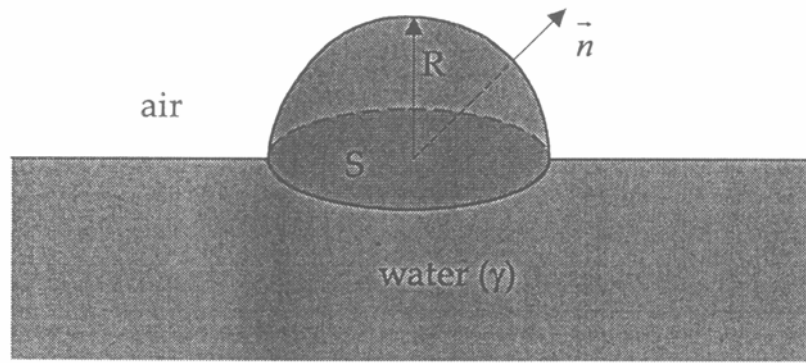


Fig. A2 Surface tension-managed spherical deformation on a liquid/air boundary

Under the bulge on the liquid surface acts the additional pressure given by the Laplace formula

$$p = 2H\gamma. \quad (\text{A13})$$

Here γ stands for the coefficient of surface tension, as always in this paper, and H is the curvature of the surface, $H=0,5(R_1^{-1}+R_2^{-1})$; R_1 and R_2 represent radii of curvatures for any couple of mutually perpendicular vertical sections in given point of the surface. Let us first look for the equation of motion of a surface particle of liquid under the restoring force of the surface tension. The layer of liquid has the length Δx , the width L , and the height Δy , as pointed out on Fig. A3.

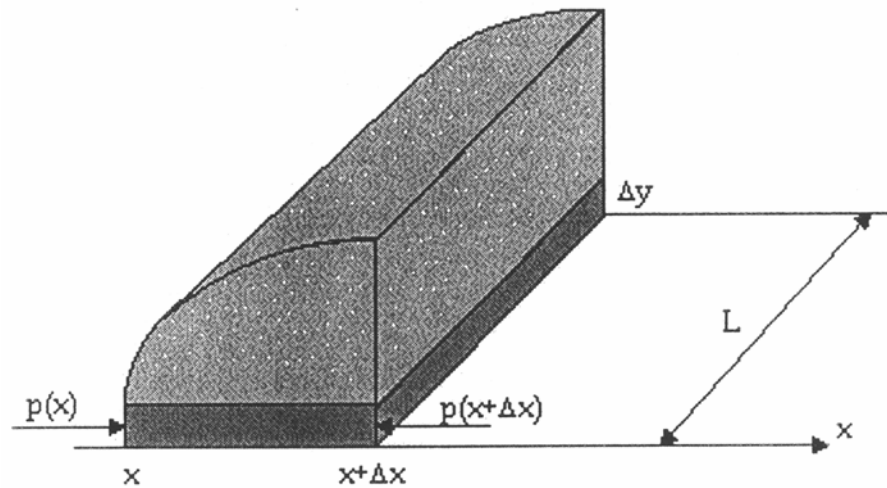


Fig. A3 Origination of restoring forces in a deformed surface layer

The resultant force in the x -direction can be evaluated from this obvious expression $F_x = [p(x+\Delta x) - p(x)] L \Delta y$, so we obtain

$$F_x = 2L\gamma \Delta x \Delta y \frac{dH}{dx}. \quad (\text{A14})$$

For small amplitudes of oscillations it is correct to approximate $2H \approx y'' = d^2 s_y / dx^2$, which gives

$$F_x = -\gamma k^3 L \Delta x \Delta y s_x. \quad (\text{A15})$$

Taking into account that the mass of the layer for a liquid of density ρ is $m = \rho \Delta x \Delta y L$, we get immediately from the force law $m s_x'' = F_x$:

$$\omega^2 = \frac{\gamma}{\rho} k^3. \quad (\text{A16})$$

This is the law of dispersion when gravitational effects can be neglected. Of course, the influence of gravity can be subsequently incorporated starting from an additional force of amount $F_x = -L\Delta y [p(x+\Delta x) - p(x)] = -L\Delta y \rho g [s_y(x+\Delta x) - s_y(x)]$ easily we arrive to the relation

$$F_x = -mgks_x. \quad (\text{A17})$$

Again from the law of force we seek the dispersion law for waves being under the dominant influence of gravity force; the result is:

$$\omega^2 = gk. \quad (\text{A18})$$

The combination of (A16) and (A18) supplies the general formula which connects the angular frequency with the wave number (a dispersion equation) in cases when neither of two effects can be neglected:

$$\omega = \sqrt{gk + \frac{\gamma}{\rho}k^3}. \quad (\text{A19})$$

It could be demonstrated (we omit details of proof; reader could consult standard courses on waves and oscillations, e.g. [3]) that this relation ought to be replaced with

$$\omega = \sqrt{\left(gk + \frac{\gamma}{\rho}k^3\right) \tanh(kh)} \quad (\text{A20})$$

for those cases when the depth of liquid in container cannot be ignored. Gravitational effects and surface tension effects dominate at low and high wave number, respectively. We can defined the crossover wave number

$$k_c = \sqrt{\frac{g\rho}{\gamma}} \quad (\text{A21})$$

in such a way that the effects are equal. The corresponding crossover frequency is

$$\omega_c = g^{\frac{3}{4}} \left(\frac{\rho}{\gamma}\right)^{\frac{1}{4}}. \quad (\text{A22})$$

We have concentrated on the frequency region where capillary effects are most important restoring forces, i.e. $\omega \gg \omega_c$. For these experiments, the wavelengths of the capillary waves are small compared to the dimensions of the container, which minimizes the effects of the container size and shape on the wave state. Parametric excitation pumps energy into waves, and as a matter of fact with the largest amplitude at $\omega = \omega_0/2$, where ω_0 is the angular forcing frequency ($\omega_0 = 2\pi F$, F being the ultrasonic transducer frequency). In typical cases of our experiments, the approximation $kh \gg 1$ is well satisfied. So, the wavelength depends only on so-called kinematical surface tension, γ/ρ , and the wave frequency:

$$\lambda = \sqrt[3]{\frac{2\pi\gamma}{\rho f^2}}. \quad (\text{A23})$$

Finally, inserting the forcing frequency of source F instead of f we readily obtain

$$\lambda = 2 \left(\frac{\gamma}{\rho} \frac{\pi}{F^2}\right)^{\frac{1}{3}} \quad (\text{A24})$$

which is the result we use throughout this paper. Let us also notice that for water in SI units $\gamma = 0.073$ and $\rho = 1000$; therefore $\lambda \approx 12.24F^{-2/3}$. Accepting a correlation factor to have a reasonable value 0.33 [4, 14] we get the convenient relation $D = 4F^{-2/3}$, as already accented in (4).

References

- [1] Bisa, Dirnagl, Esche, *Zerstäubung von Flüssigkeiten mit Ultraschall*, Siemens Zeitschr., 8, (1954), 341-347.
- [2] S. Ciliberto, and J. Gollub, *Chaotic mode competition in parametrically forced surface waves*, J. Fluid Mech., **158**, (1985), 381.
- [3] F. S. Crawford, *Waves* (Berkeley Physics Course, Volume 3), McGraw-Hill Book Company; Russian edition, Moscow 1984, 308-314. See also: L. D. Landau and E. M. Lifshitz, *Fluid Mechanics*, Pergamon Press, New York, 1987.
- [4] W. D. Drews, *Flüssigkeitszerstäubung durch Ultraschall*, Elektronik – München, 10, (1979), 83-86.
- [5] W. D. Drews, *Kavitation durch Beschallung dünner Kavitation Flüssigkeitsschichten mit piezoelektrischen Ultraschall-Biege-schwingern*, Metal, 1, (1979), 41-49.
- [6] W. Eisenmenger, *Dynamic Properties of the Surface Tension of Water and Aqueous Solutions of Surface Active Agents with Standing Capillary Waves in the Frequency Range from 10kc/s to 1.5Mc/s*, Acoustica, 9, (1959), 327-340.
- [7] Esche, *Erzeugung von Hochwertigen Aerosollen Mittels Ultraschall*, Communicat. congrès, Marseille, (1955), 179-183.
- [8] E. L. Geršenzon, O. K. Eknadiosjanc, *On Nature of Liquid Atomization in Ultrasonic Fountains* (in Russian), Acoustic Journal, X, 2, (1964), 158-162.
- [9] C. L. Goodridge, W. Tao Shi, and D. P. Lathrop, *Threshold Dynamics of Singular Gravity-Capillary Waves*, Phys. Rev. Lett., **76**, (1996), 1824.
- [10] C. L. Goodridge, W. Tao Shi, H. G. E. Hentschel, and D. P. Lathrop, *Viscous effects in droplet-ejecting capillary waves*, Physical Review E, **56**, 1, (1997), 472-475.
- [11] C. L. Goodridge, H. G. E. Hentschel, and D. P. Lathrop, *Breaking Faraday Waves: Critical Slowing of Droplet Ejection Rates*, Physical Review Letters, **82**, 15, (1999), 3062-3065.
- [12] R. J. Lang, *Ultrasonic Atomization of Liquids*, The Journal of the Acoustical Society of America, **34**, 1, (1962), 6-8.
- [13] A. M. Prohorov (Editor-in-Chief), *Encyclopedia of Physics* (in Russian), 'Soviet encyclopedia', Tom 2, Moscow 1988, s. 228.
- [14] D. Šarković, *Ultrasonic Atomization of Liquids* (in Serbian), M. A. Thesis, Faculty of Electrical Engineering, Ljubljana 1985..24
- [15] M. Topp, P. Eisenklam, *Industrial and Medical Uses of Ultrasonic Atomizers*, Ultrasonics, (1972), 127-133.
- [16] R. W. Wood, A. L. Loomis, *The Physical and Biological Effects of High Frequency Waves of Great Intensities*, Phil. mag., 4, 22, (1927), 417-436.